

**NASA TECHNICAL
MEMORANDUM**



NASA TM X-2733

NASA TM X-2733

**EXPERIMENTAL INVESTIGATION
OF AERODYNAMIC PERFORMANCE
OF COOLED TURBINE VANES AT
GAS- TO COOLANT-TEMPERATURE
RATIOS UP TO 2.75**

by Roy G. Stabe and Robert P. Dengler

Lewis Research Center

Cleveland, Ohio 44135

1. Report No. NASA TM X-2733		2. Government Accession No.		3. Recipient's Catalog No.	
4. Title and Subtitle EXPERIMENTAL INVESTIGATION OF AERODYNAMIC PERFORMANCE OF COOLED TURBINE VANES AT GAS- TO COOLANT-TEMPERATURE RATIOS UP TO 2.75				5. Report Date March 1973	
				6. Performing Organization Code	
7. Author(s) Roy G. Stabe and Robert P. Dengler				8. Performing Organization Report No. E-7183	
9. Performing Organization Name and Address Lewis Research Center National Aeronautics and Space Administration Cleveland, Ohio 44135				10. Work Unit No. 501-24	
				11. Contract or Grant No.	
				13. Type of Report and Period Covered Technical Memorandum	
12. Sponsoring Agency Name and Address National Aeronautics and Space Administration Washington, D.C. 20546				14. Sponsoring Agency Code	
15. Supplementary Notes					
16. Abstract The results of an experimental investigation of the aerodynamic performance of two geometrically similar turbine vanes with different cooling designs are presented. The test vanes were a convection-film-cooled vane and a transpiration-cooled vane. A solid uncooled vane with the same aerodynamic profile as the cooled vane was also tested. Four vanes of each type were tested in an annular sector cascade. The cooled vanes were tested at primary to coolant temperature ratios of 1.0, 1.75, and 2.75 and a coolant to primary pressure ratios of 1.0, 1.2, and 1.5. This resulted in coolant flows up to about 10 percent of the primary flow. The principal measurements were surveys of vane exit total pressure, total temperature, and static pressure. The report includes a brief description of the test facility and the design of the test vanes. The test results presented include weight flow and efficiency data for the uncooled vanes and coolant flow, primary flow, and efficiency data as functions of the cooling variables for the cooled vanes.					
17. Key Words (Suggested by Author(s)) Jet engine Blade cooling Turbine Performance Turbine blades High temperature			18. Distribution Statement Unclassified - unlimited		
19. Security Classif. (of this report) Unclassified		20. Security Classif. (of this page) Unclassified		21. No. of Pages 32	
				22. Price* \$3.00	

Page Intentionally Left Blank

EXPERIMENTAL INVESTIGATION OF AERODYNAMIC PERFORMANCE OF COOLED TURBINE VANES AT GAS- TO COOLANT-TEMPERATURE RATIOS UP TO 2.75

by Roy G. Stabe and Robert P. Dengler

Lewis Research Center

SUMMARY

The results of an experimental investigation of the aerodynamic performance of two geometrically similar turbine vanes with different cooling designs are presented. The test vanes were a convection-film-cooled vane and a transpiration-cooled vane. Four vanes of each type were tested in an annular sector cascade. The cooled vanes were tested at primary to coolant temperature ratios of 1.0, 1.75, and 2.75 and at coolant to primary pressure ratios of 1.0, 1.2, and 1.5. This resulted in coolant flows up to about 10 percent of the primary flow. The principal measurements were surveys of vane exit total pressure, total temperature, and static pressure.

The convection-film-cooled vane ejected the coolant from film cooling slots on the pressure and suction surfaces and also from a trailing edge slot. Since the coolant was ejected substantially in the direction of the primary flow, the energy of the coolant could add to the output of the vane. The transpiration-cooled blade ejected the coolant over most of the blade surface and in a direction normal to that of the primary flow so that the energy of the coolant could not be effectively utilized. These differences significantly affected the aerodynamic performance of the test vanes.

The primary efficiency of the convection-film-cooled vane increased with increased coolant flow and was also dependent on the primary to coolant temperature ratio. The primary efficiency was higher at a temperature ratio of 1.0 where the energy of the coolant relative to the energy of the primary flow was highest. The primary efficiency of the transpiration-cooled vane decreased with increasing coolant and was not dependent on the temperature ratio. At a coolant to primary pressure ratio of 1.0 and a primary to coolant temperature ratio of 2.75, the percent coolant flows for both cooled vanes were approximately the same as 3.5 percent. But the primary flow for the transpiration-cooled vane was 7.0 percent less than it was for the uncooled vane. At these same flow conditions the primary and thermodynamic efficiencies for the convection-film-cooled vane were 0.951 and 0.939, respectively. The comparable figures for the transpiration-cooled vane were a primary efficiency of 0.918 and a thermodynamic efficiency of 0.907.

INTRODUCTION

The use of higher turbine inlet temperatures in modern aircraft engines has necessitated increasingly comprehensive and sophisticated turbine cooling schemes. The general method of cooling the turbine is to direct relatively cool air bled from the compressor through the turbine blading. This cooling air is then ejected into the primary gas stream. Such ejection can adversely affect the aerodynamic performance of the turbine.

Several investigations of the effect of cooling on turbine performance have been performed at NASA's Lewis Research Center. Reference 1 summarizes much of this work. And an analysis of the effect of several cooling variables on turbine performance is presented in reference 2. However, the experimental work was done with ambient temperature primary and coolant air. More information at primary gas temperatures and primary to coolant gas temperature ratios more representative of modern engines is needed.

This report presents the results of an experimental investigation of the aerodynamic performance of two geometrically similar turbine vanes with very different cooling designs. These were a convection-film-cooled vane and a transpiration-cooled vane. A solid, uncooled vane with the same aerodynamic design as the cooled vanes was also tested to provide a base point for comparison of the cooled vane performance. Four vanes of each type were tested in an annular sector cascade. The tests of the cooled vanes were conducted with primary gas temperatures ranging from ambient to 812 K (1000° F). Performance data were obtained at primary gas to coolant temperature ratios of approximately 1.00, 1.75, and 2.75 and at coolant to primary pressure ratios of 1.0, 1.2, and 1.5. This resulted in a range of coolant flow up to about 10 percent of the primary flow. The principal measurements were surveys of the vane exit total pressure, total temperature, and static pressure.

This report includes a brief description of the test facility and the design of the cooled vanes. The test results presented include weight flow and efficiency data for the uncooled vane and coolant flow, primary flow, and efficiency data as functions of the cooling variables for the cooled vanes.

SYMBOLS

- p absolute pressure, N/cm^2 (lbf/in.²)
- T temperature, K (°F)
- V velocity, m/sec (ft/sec)
- w weight flow, kg/sec (lbm/sec)

Y	ratio of coolant flow to primary flow, w_c/w_p
α	flow angle
δ	ratio of inlet total pressure to U. S. standard sea-level atmospheric pressure, $p'_1/10.132 \text{ N/cm}^2$ ($p'_1/14.696 \text{ lb/in.}^2$)
η	efficiency
$\sqrt{\theta}_{cr}$	ratio of inlet primary critical velocity to critical velocity of U. S. standard sea-level air, $V_{cr,p}/310.6$ ($V_{cr,p}/1019.2$)

Subscripts:

c	coolant flow
cr	flow conditions at Mach 1
eq	equivalent to inlet conditions with U. S. standard sea-level air
id	ideal or isentropic process
p	primary flow
t	thermodynamic
uc	uncooled vane
1	station at vane inlet
2	station at vane exit or survey plane
3	station at vane exit where flow conditions are assumed uniform

Superscript:

'	total state condition
---	-----------------------

APPARATUS AND PROCEDURE

Cascade Facility

The cascade test rig used for this investigation was basically the same as that described in references 3 and 4. Briefly, the rig consisted of five major components; an inlet section, a burner section, a circular-to-annular cross section transition section, the test section, and an exit section. This cascade test unit was designed and fabricated for conducting heat transfer tests and was not originally intended for use as an aerodynamic test vehicle. For the tests described herein, some modifications to the basic test rig were required. The exit section was replaced with another section of the same general geometry but incorporating a pressure and temperature survey rake. In addition,

the high-temperature burner section and inlet section were removed and replaced with a simple spool piece. Figure 1 illustrates the basic cascade test unit as it was used for these tests. An auxiliary system upstream of the basic cascade test unit incorporated a low-temperature burner which was used for heating the primary flow to the cascade test unit. This burner was operated on natural gas. Figure 2 shows the general location of the low-temperature burner with respect to the test unit and illustrates the combustion air flow path for these tests.

The test section represented an annular sector of a vane row and contained four vanes and five gas flow channels. Four vanes of the same cooling design were assembled together as a vane pack before being inserted into the test section. Figure 3 shows a typical assembled pack of the convection-film-cooled vanes. The cooling air entered the vane proper through an inlet tube at the outer radius (tip) of the vanes. Cooling air for all four vanes was supplied from a common plenum just outside the cascade test section. A top view of the test section is shown in figure 4 with the access cover removed and a vane pack assembly inserted in place.

Vanes having two different cooling designs, but with a common external profile, were tested during this investigation. A solid, uncooled vane with the same aerodynamic design as these cooled vanes was also tested for reference purposes. The external vane profile is of a twisted design and is defined by the coordinates and dimensional information presented in table I. Coordinates are given for the vane external profile at three radial sections defined as B-B, C-C, and D-D. The vane has a span of 9.78 centimeters (3.85 in.), an axial chord of 5.08 centimeters (2.00 in.) at the mean radius, and a spacing of 3.10 centimeters (1.22 in.) at the mean radius resulting in a vane axial solidity of 1.64. The two cooled designs provided for all or most of the coolant to be discharged through the vane skin or shell and into the primary gas stream. Figure 5(a) shows the vane that incorporates film cooling slots and a slotted trailing edge. Figure 5(b) shows the transpiration-cooled vane.

Figure 6 presents cross-sectional view of the convection-film-cooled vane (fig. 5(a)) and illustrates the internal coolant flow configuration. Cooling air entering the inlet supply tube at the vane tip (outer radius) flows into a vane tip plenum chamber at which point the flow then divides. A portion of the air flows into a spanwise tube located near the vane leading edge. From here the air flows through spanwise slots in this tube to impinge on the internal surface of the leading edge. This coolant then further divides, flows rearward along the pressure and suction surface to a common region, and then flows radially inward (towards the vane hub) and exits beneath the vane. This expelled coolant subsequently discharges into the gas stream downstream of the vane row and exit measuring station. The remaining cooling air in the vane tip plenum is directed to a midchord supply chamber that separates the pressure surface from the suction surface. Cooling air from this chamber then flows through small holes in the walls of the midchord supply chamber to impinge on the internal surfaces of the vane's suction and

pressure sides, and subsequently flows rearward. Some of this air is then discharged into the gas stream at a shallow angle through film cooling slots on both the pressure and suction surfaces (see fig. 6) and the remainder is expelled into the gas stream through a slotted trailing edge. Cooling air from the film cooling slots on the pressure surface exits at an average angle of about 18 degrees with respect to a surface tangent, and about 12 degrees for air exiting from the film cooling slots on the suction surface.

Figure 7 presents cross-sectional views of the transpiration-cooled vane of figure 5(b) and illustrates the internal coolant flow configuration. The basic design consists of a cast fluted internal strut with a wire-form porous shell attached to it. The porous shell material is constructed by winding flattened wire 0.005 by 0.025 centimeter (0.002 by 0.010 in.) on a mandrel to obtain overlays angled at about 60° to the previous layer. Nine overlays were used to obtain a vane shell thickness of about 0.061 centimeter (0.024 in.). This results in a uniform pore size of about 0.0025 centimeter (0.001 in.). This sheet material was then formed to the desired external vane profile and fitted to the cast fluted strut with the two edges of the material coming together at the vane trailing edge. An electron beam welding process was used to join the trailing edge and also to attach the shell to the lands of the fluted strut (see fig. 5(b)).

Cooling air entering the inlet supply tube flows into a vane tip plenum similar to that described for the film-cooled vane of figure 6. Metering orifices are provided at the entrance of each of the chambers formed by the fluted strut and the vane shell. After flowing through the orifices and into the separate chambers, the air then transpires through the porous shell to provide a most effective cooling method.

Instrumentation

Figure 8 shows schematics of the top and side views of the cascade test section and indicates the general location of instrumentation used in this investigation. Two actuated probes were located at the inlet to the vane row (station 1) for measuring total temperature and total pressure. A static pressure tap was also located at this station. Symbols on the figure indicate the locations where the particular measurements were made. At the exit of the vane row (station 2) an actuated rake was used to obtain a survey of total temperature, total pressure, and static pressure for the various flow conditions tested. As depicted in the side view, there are a total of 15 measuring elements; seven for measuring temperatures, six for measuring total pressures, and two for measuring static pressures. The pressure probes for this rake were made from 0.16 centimeter (0.062 in.) o.d. stainless-steel tubing having a wall thickness of 0.030 centimeter (0.012 in.). The two static pressures were measured through the use of wedge heads installed at the end of the 0.16-centimeter tubing. As shown in the inset of the figure, the wedge had an included angle of 15° . Temperature measurements from

this rake were made with 0.16 centimeter (0.062 in.) o.d. sheathed Chromel-Alumel thermocouple assemblies. The actual wire size in these assemblies is 0.025 centimeter (0.010 in.) diameter. Six static pressure taps, three on the outer radius and three on the inner radius, are also provided at station 2. These taps are so located as to measure pressures in the midstream at the exit of flow channels 2, 3, and 4 (see fig. 8(a)).

As stated previously, the four vane cascade represented an annular sector. The exit survey rake incorporated in the replacement exit section designed for these tests, however, was actuated in a direction that was perpendicular to the vertical centerline of the cascade inlet. This vertical centerline also coincided with the stacking line (see point Z of table I) of vane 3. The direction of rake movement is shown in figure 8(a). The rake probes were all positioned at an angle of 64° with respect to the cascade inlet flow direction, and this corresponds to the cascade free stream exit flow angle for the vanes at the vane mean radius. Figure 9 is a schematic depicting the cascade exit and illustrates the relative location of vane trailing edges with respect to the survey rake probe elements along its travel. The view is looking upstream in a direction parallel to the inlet flow.

Additional instrumentation, as described in reference 3, was used for obtaining operational measurements. Measurements of particular interest are those for determining primary gas stream and test vane coolant flow rates. Combustion air supplied to the auxiliary system was measured with a Venturi flowmeter and combustion air flowing through the bypass line was measured with an orifice (see fig. 2). Cooling air flow to the test vanes was measured with a Venturi located upstream in the cooling air supply line (not shown in fig. 1 or 2). The cooling air pressure and temperature were measured in the plenum just outside of the cascade rig test section (see fig. 1).

Procedure

Combustion air at a pressure of 86.2 N/cm^2 (125 psia) was supplied to the cascade rig from a laboratory source, and the test conditions were set by controlling inlet total pressure and temperature and the exit static pressure. Test conditions at the inlet to the cascade vane row were maintained through monitoring the total pressure and temperature probes positioned at the vane mean radius (midspan) at station 1. All tests were conducted at an inlet total pressure of 31.0 N/cm^2 (45 psia). This inlet pressure was controlled primarily by a throttling valve upstream of the vane row (see fig. 2). The pressure ratio across the vanes (or exit static pressure) was controlled by an exhaust control valve downstream of the vane row.

Testing was conducted at three different nominal cascade inlet temperatures; namely, 300, 532, and 812 K (80° , 500° , and 1000° F). The cooling air temperature for

the majority of the cooled tests was 300 K (80° F) which resulted in nominal primary to coolant temperature ratios of 1.00, 1.75, and 2.75.

Some testing was also done at a cascade inlet temperature of 812 K (1000° F) with cooling air that was heated to a temperature of 464 K (374° F). This results in a primary to coolant temperature ratio of about 1.75. For all the cooled tests, cooling air was supplied to the vanes at coolant to inlet gas pressure ratios p'_c/p'_p of 1.0, 1.2, and 1.5.

The design value for the exit ideal critical velocity ratio $(V/V_{cr})_{id,3}$ for these vanes at the mean radius was 0.87. Tests for the uncooled (solid) vane were conducted over a range of exit ideal critical velocity ratios from approximately 0.72 to 0.91 while testing of the cooled vane configurations was conducted only at the design ideal critical velocity ratio. The inlet-total to exit-static pressure ratio was used to determine and set the desired exit ideal critical velocity ratios. The three vane, hub and tip static pressures at station 2 were averaged to obtain a representative value for the exit mid-span static pressure.

A total and static pressure and total temperature survey was made with the exit rake for each set of test conditions. The total rake travel for each survey was 6.25 centimeters (2.45 in.), which covered the wakes of the two middle vanes of the four-vane pack as illustrated in figure 8. Each survey was made by recording data at 49 points resulting in 48 equal increments of rake travel; each increment of rake travel therefore being approximately 0.13 centimeter (0.051 in.). The output signals of the thermocouples and transducers were automatically digitized and recorded on magnetic tape.

Data Reduction

The performance results presented in this report were calculated from the exit survey measurements. The data required for these calculations were: the vane exit total pressure p'_2 , total temperature T'_2 , static pressure p_2 , flow angle α_2 , and probe position. Twenty-five data points for each of the six total pressure probes between the static pressure wedge probes (see figs. 8 and 9) were used for these calculations. This data encompassed one vane wake and a vane to vane distance equal to one mean diameter vane pitch. Each set of 25 consecutive data points was selected from the 49 points recorded so that the wake was approximately centered in the set. This was done because each probe on the rake intercepts the wake at a different location in the vane to vane direction. This occurs because radial variation of velocity and flow angle result in displacement of the wake at the plane of the rake, station 2 (see fig. 9). Total temperature and static pressure were then determined for each of the six total pressure probes by linear interpolation of the data from the total temperature and static pressure probes.

The flow angle was assumed to be equal to the velocity diagram angle at the radius of each total pressure probe.

The flow angle and pressure and temperature measurements were used to calculate velocity, mass flow, and the tangential and axial components of momentum for each of the six total pressure probes and each of the 25 data cycles. These quantities were then integrated numerically to obtain overall values at the plane of the rake, station 2. The area of integration was a parallelogram with a base dimension equal to one mean diameter vane pitch, 3.11 centimeters (1.224 in.) and a height equal to the span of the six total pressure probes, 4.60 centimeters (1.813 in.) (see fig. 9).

The continuity and conservation of momentum and energy relations were then used to calculate the flow angle, velocity, pressures and temperatures at a hypothetical location where the flow conditions were assumed uniform. This location is designated station 3. For these calculations, a constant area process and conservation of the tangential component of momentum were assumed between stations 2 and 3. The results presented in this report are based on the aftermix conditions calculated for station 3. They are only for a region in the center of the vane span and do not include end wall losses.

The inlet total conditions of the primary flow, p'_p and T'_p , were determined by averaging several data points measured in the free-stream by each probe on the survey rake.

The efficiency for the uncooled vane is defined as

$$\eta_{3,uc} = \left(\frac{V_3}{V_{id,p}} \right)^2 \quad (1)$$

Two efficiencies are used for the cooled vanes. These are the primary efficiency $\eta_{3,p}$ and the thermodynamic efficiency $\eta_{3,t}$. The primary efficiency is defined as the ratio of the actual vane output to the ideal output of the primary flow only; that is,

$$\eta_{3,p} = \frac{(w_p + w_c)V_3^2}{w_p V_{id,p}^2} \quad (2)$$

where V_3 is the actual velocity of the primary and coolant flows after they have mixed and $V_{id,p}$ is the velocity for an isentropic process between the inlet or primary total pressure and temperature and the aftermix static pressure p_3 .

The thermodynamic efficiency is defined as the ratio of the actual vane output to the ideal output of both the primary and coolant flow; that is,

$$\eta_{3,t} = \frac{(w_p + w_c)V_3^2}{w_p V_{id,p}^2 + w_c V_{id,c}^2} \quad (3)$$

where $V_{id,c}$ is the velocity for an isentropic process between the coolant supply total pressure and temperature and the aftermix static pressure.

These efficiencies can also be expressed in terms of the ratio of the square of the aftermix velocity V_3^2 to the square of the ideal velocity of the primary flow $V_{id,p}^2$ and the ratio of coolant flow to primary flow Y .

$$\eta_{3,p} = (1 + Y) \left(\frac{V_3}{V_{id,p}} \right)^2 \quad (4)$$

$$\eta_{3,t} = \frac{(1 + Y) \left(\frac{V_3}{V_{id,p}} \right)^2}{1 + Y \left(\frac{V_{id,c}}{V_{id,p}} \right)^2} \quad (5)$$

The term $(V_{id,c}/V_{id,p})^2$ is the ratio of the ideal kinetic energy of the coolant to that of the primary flow.

RESULTS AND DISCUSSION

The results of the experimental investigation are presented in three sections. First, the results of the uncooled (base) vane investigation are discussed. The next two sections discuss results from the film-cooled vane and the transpiration-cooled vane, respectively. Corresponding samples of the wake survey measurements and plots of weight flow and vane efficiency are included and compared.

Uncooled Vane

The uncooled vane was tested over a range of ideal exit critical velocity ratios of approximately 0.72 to 0.91 with ambient gas temperature. The mean radius design ideal exit velocity ratio was 0.87. This vane was also tested over a smaller range of

exit velocity ratios at gas temperatures of approximately 532 and 812 K (500° and 1000° F). These tests provide a base point for comparison of the cooled vane performance.

Samples of the exit survey data for gas temperatures of approximately 300 K (80° F), 532 K (500° F), and 812 K (1000° F) are shown in figures 10(a), (b), and (c), respectively. In figure 10, every fourth data point is shown with a symbol. The data shown in figure 10 are for a pressure probe near the vane midspan and for an exit ideal critical velocity ratio $(V/V_{cr})_{id,3}$ near the design value. The total pressure wake tends to become shallower and wider with increasing gas temperature. However, these changes are quite small and may not have a significant effect on efficiency.

The integrated equivalent weight flow and the aftermix efficiency are shown as functions of exit velocity ratio in figures 11(a) and (b), respectively. As expected, the equivalent flow does not seem to be significantly dependent on temperature. The efficiency, however, does vary with temperature but not in an orderly manner. The mean value of efficiency corresponds roughly with the ambient temperature data. At gas temperatures of 532 K (500° F), the efficiency is about one-half percentage point higher than the mean and is about one-half percentage point lower than the mean at gas temperatures of 812 K (1000° F). The reason for this kind of variation is not known. The uncooled vane efficiency decreases gradually with increasing exit velocity ratio. At design ideal exit critical velocity ratio (0.87), the mean efficiency is 0.954.

Convection-Film-Cooled Vane

The cooling configuration of this vane was described in the test vane section. This vane was tested at approximately design exit velocity ratio (0.87) and over a range of primary to coolant total temperature ratios and coolant to primary total pressure ratios.

Coolant flow. - The coolant flow rate as a percentage of the primary flow (the flow entering the blade row) is shown as a function of the coolant to primary pressure ratio and primary to coolant temperature ratio in figures 12. A different symbol is used for each pressure-temperature ratio combination. These same symbols are used for similar combinations throughout this report. Figure 12(a) shows the total coolant flow. Figure 12(b) shows the coolant flow with the leading edge impingement coolant supply (see fig. 6) closed off. The data shown in figure 12(b) is the coolant flow which is injected into the primary flow stream. It is presented here because it may be helpful in analyzing losses due to injecting coolant into the primary flow. The data presented in this report are based on the total coolant flow as shown in figure 12(a).

Figure 12(a) shows that the percent coolant flow increases with both temperature and pressure ratio. The increase in the percent coolant flow with temperature ratio is

due to the relatively greater density of the coolant as the temperature of the primary flow increases. At a constant pressure ratio, the percent coolant increases approximately with the square root of the temperature ratio. This should be the case if the coolant flow is constant with coolant to primary pressure ratio. Comparison of figures 12(a) and (b) indicates that with the leading edge cooling passage blocked, approximately 80 to 85 percent of the total coolant flow is injected through the cooling slots into the primary flow. About 50 percent of the total coolant is ejected through the trailing edge slot.

Most of the data shown in figure 12 is for ambient temperature coolant and either ambient or heated primary flow. The half solid symbols shown in figure 12(a) are for 812 K (1000° F) primary flow and heated coolant for a primary to coolant total temperature ratio of 1.75. These data agree very well with the ambient temperature data.

Reduction of primary flow. - When coolant is injected into the primary flow stream from the vane surfaces, and the pressure ratio across the vane row is constant, it usually reduces the primary flow rate. This reduction is effected through blockage - making part of the flow area unavailable to the primary flow or through interference with the primary flow process and increased loss.

The reduction in equivalent primary flow, as a percentage of the uncooled vane flow, is shown in figure 13 as a function of percent coolant flow and pressure and temperature ratio. The primary flow decreases with increasing percent coolant flow. This decrease becomes larger as the primary to coolant total temperature ratio increases. The rate of primary flow decrease, however, is nearly the same for all three temperature ratios at about 1 percent for each percent coolant flow up to a pressure ratio of 1.2. This rate increases sharply to about 2 percent per percent coolant at a pressure ratio of 1.5 for temperature ratios of 1.75 and 2.75.

Exit surveys. - Exit survey data for three pressure ratios and three temperature ratios are shown in figure 14. The example data shown are for a pressure probe near the vane midspan and were obtained at approximately design exit ideal critical velocity ratio.

This figure shows that there is a total temperature wake as well as a total pressure wake at primary to coolant temperature ratios greater than unity. The size of this temperature wake increases with both pressure and temperature ratio, that is, it increases with percent coolant flow. This wake will result in lower velocities and therefore represents additional loss in both efficiency and flow.

The depth of the total pressure wake trace decreases with increasing coolant flow. These particular vanes employ a trailing edge slot through which a large portion (about 50 percent) of the coolant flows into the vane wake. It was shown in reference 1 that trailing edge coolant ejection can reduce the size of the wake and also the loss. This is what seems to be happening in this case. The coolant flowing from the trailing edge slot

reduces the size of the total pressure wake but in so doing it increases the size of the total temperature wake.

There is also a small variation in the width of the total pressure wake with coolant pressure and temperature ratio. This variation is probably the result of the coolant flowing from the pressure and suction surface film cooling slots (see fig. 6).

Efficiency. - The primary and thermodynamic efficiencies are presented as functions of percent coolant flow and primary to coolant total temperature ratio and coolant to primary total pressure ratio in figure 15. The primary efficiency increases with increasing coolant flow and is also dependent on the primary to coolant temperature ratio. The highest primary efficiency and also the highest rate of increase of efficiency with coolant flow occur at a temperature ratio of 1.0. The primary efficiency reflects the output of the mixed primary and coolant flow per unit of primary flow. The primary efficiency can therefore increase even though the kinetic energy of the mixed flow is decreasing because the mixed flow is larger than the primary flow. Equation (3) shows that the primary efficiency increases with percent coolant flow as long as the rate of decrease of aftermix kinetic energy is less than 1.0 percent per percent coolant flow.

The convection-film-cooled vanes were designed to eject the coolant substantially in the direction of the primary flow. When this is the case, the energy of the coolant, even when its energy is less than the energy of the primary flow, can add to the output of the vane or at least reduce the loss due to mixing the lower velocity and temperature coolant with the primary flow. A comprehensive discussion of the effects of coolant temperature, velocity, direction, and location of injection on turbine blade performance can be found in reference 2.

The dependence of primary efficiency on the primary to coolant total temperature ratio is apparently due to the difference in the energy of the coolant relative to the primary flow at the various temperature ratios. The ideal energy of the coolant relative to the primary flow is highest at a temperature ratio of one and increases with coolant to primary total pressure ratio. At temperature ratios greater than one, the ideal energy of the coolant was less than the ideal energy of the primary flow at all of the coolant to primary total pressure ratios investigated.

The efficiency for the uncooled vane and for the cooled vane with no coolant flow is also shown in figure 15. The efficiency of the uncooled vane is almost one point higher than the efficiency of the cooled vane at zero flow. This difference in efficiency occurs because pressure on the pressure surface of the vane is high enough so that, at zero or very low coolant flow rates, the primary flow can flow into the pressure surface film-cooling slot and flow out of the trailing edge and suction surface slots. This results in a loss in efficiency. The data for a primary to coolant temperature ratio of 1.75 with heated coolant (half-filled symbols) is in reasonably good agreement with the data for ambient temperature coolant.

The thermodynamic efficiency decreases with increasing percent coolant flow. Also, the variation of this efficiency with the primary to coolant total temperature ratio is the reverse of what it was for the primary efficiency. For a given coolant flow, the highest thermodynamic efficiencies occur at the highest primary to coolant total temperature ratio or where the energy of the coolant is lowest relative to the energy of the primary flow. This reverse occurs because the thermodynamic efficiency is based on the ideal energy of both the primary and the coolant flows. And, in this case, the ideal energy of the coolant was much greater than the increase in output actually realized from the energy of the coolant.

Transpiration-Cooled Vane

The cooling configuration of this vane was described in the test vane section. This vane was tested at approximately design exit velocity ratio and at coolant to primary total pressure ratios of 1.0, 1.2, and 1.5 at primary to coolant total temperature ratios of 1.00, 1.78, and 2.76 with ambient temperature coolant. This vane was also tested with heated coolant with a primary gas temperature of about 812 K (1000° F) so that the ratio of primary to coolant total temperatures was 1.78.

Coolant flow. - The coolant flow rate as a percentage of the primary flow is shown as a function of the coolant to primary total pressure ratio and primary to coolant total temperature ratio in figure 16. The coolant flow rates shown in this figure are somewhat higher than they were for the film-cooled vane (see fig. 12), but the variation with pressure and temperature ratio is similar. With heated coolant, however, the coolant flow rate was less than with the ambient temperature coolant. The most significant difference occurred at a pressure ratio of 1.5 where the coolant flow was 7 percent of the primary flow with heated coolant compared to 8 percent with ambient temperature coolant.

Reduction of equivalent primary flow. - The change in primary flow, as a percentage of the uncooled vane flow, is shown as a function of percent coolant flow in figure 17. The change in primary flow for the transpiration-cooled vane is not dependent on temperature ratio as it was for the film-cooled vane. Also, the reduction in primary flow is larger and the primary flow decreases more rapidly with percent coolant flow than it did for the film-cooled vane. The primary flow decreases with increasing coolant flow at a rate of about 2 percent per percent coolant flow over most of the range of coolant flow. For the film-cooled vane, the primary flow decreases at a rate of about 1.0 percent per percent coolant flow. At a coolant to primary pressure ratio of 1.0 and a primary to coolant temperature ratio of 2.76 the primary flow was 7 percent less than it was for the uncooled vane and the coolant flow was 3.5 percent of the primary flow. The total flow (primary plus coolant) then, was about 3.5 percent less than for the uncooled vane. The corresponding figures for the film-cooled blade were a 4.4 percent reduction

in primary flow with a coolant flow of 3.6 percent of the primary (see fig. 13). In this case the total flow was only 0.8 percent less than for the uncooled vane.

Exit surveys. - Exit survey data for the three pressure ratios and three temperature ratios investigated are shown in figure 18. These data are for a pressure probe near the vane midspan and at approximately design exit ideal velocity ratio.

Both the total temperature and the total pressure wakes are larger for this vane than they were for the film-cooled vane (see fig. 14). This is an indication that the losses are also larger. The total temperature wake increases in size with both coolant pressure and temperature ratio for coolant to primary pressure ratios greater than one. That is, it increases with percent coolant flow as was the case for the film-cooled vane. The size of total pressure wake also increases with the coolant to primary pressure ratio. This wake, however, gets shallower as the primary to coolant temperature ratio increases to 2.76. The reason for this is not clear; however, this is not the same effect as was noted for the film-cooled vanes. In that case, the size of the total pressure wake decreased uniformly with increased percent coolant flow. And this was attributed to filling of the wake by coolant ejected from the trailing edge slot. The differences in the size of the total pressure wakes for the film- and transpiration-cooled vanes are apparently due to the manner in which the coolant is injected into the primary flow. In the film-cooled vane the coolant is ejected through a few slots substantially in the direction of the primary flow. In the transpiration-cooled vane the coolant is ejected over the entire surface and in a direction normal to the primary flow. This could result in an accumulation of low momentum fluid along the vane surfaces which would result in a larger wake.

Efficiency. - The primary and thermodynamic efficiencies of the transpiration-cooled vanes are shown as a function of percent coolant flow in figure 19. The primary efficiency differs in several respects from the primary efficiency for the convection-film-cooled vane (see fig. 15). It is considerably lower. It decreases as the coolant flow increases. And it is not clearly dependent on the temperature ratio. All of these effects are probably due to the manner in which the coolant was injected into the primary flow. The coolant was injected from the entire blade surface in a direction normal to the direction of the primary flow. The kinetic energy of the coolant, then, was not available to add to the output of the vane as it was for the film-cooled vane. Also, the accumulation of low momentum fluid on the vane surfaces would lead to larger loss.

The primary efficiency for a pressure ratio of 1.0 and a temperature ratio of 2.76 (diamond symbol in fig. 19) is 0.918 compared to 0.951 for the film-cooled vane at similar conditions and 0.954 for the uncooled vane. The data for heated coolant at a temperature ratio of 1.78, represented by the half-filled symbols in figure 19, agree fairly well with the ambient temperature data even though the coolant flows were lower.

The primary efficiency decreases with increasing coolant flow at an average rate of about 0.7 points in efficiency per percent coolant flow. According to equation (4) this is

an indication that the kinetic energy of the mixed flow decreases with coolant flow. This probably occurred because the energy of the coolant added very little to the output of the vane. Reference 2 indicates that the primary efficiency decreases at a rate of 1.0 percent per percent coolant flow when the net energy of the coolant relative to the primary flow, before mixing, is zero.

There is some variation in the primary efficiency with temperature ratio. But this variation is not systematic. The mean value of primary efficiency corresponds approximately to the data for a coolant to primary temperature ratio of 2.76. The data for a temperature ratio of 1.0 is somewhat higher than the mean and the data for a temperature ratio of 1.78 is somewhat lower. This variation is probably scatter due to some inconsistencies in the data. The variation should be small, however, because the energy of the coolant is not available to the mixing process.

The thermodynamic efficiency for the transpiration-cooled vanes is also shown in figure 19. This efficiency decreases very rapidly with increased coolant flow. At a temperature ratio of 2.76 and a pressure ratio of 1.0 the thermodynamic efficiency is 0.907. The thermodynamic efficiency decreases to 0.825 at a pressure ratio of 1.5. The thermodynamic efficiency for the film-cooled vane for similar conditions decreased from 0.939 to 0.916. The thermodynamic efficiency varies with temperature in the same way as for the film-cooled vane. This variation occurs because the thermodynamic efficiency is based on the ideal energy of both the primary and coolant flows. And the ideal energy of the coolant relative to the primary flow is dependent on the temperature and pressure ratios.

SUMMARY OF RESULTS

The aerodynamic performance of two geometrically similar turbine vanes with different cooling designs was investigated experimentally in an annular sector cascade. The vanes were tested at approximately design ideal exit critical velocity ratio and over a range of coolant flows and at primary to coolant temperature ratios of 1.0, 1.75, and 2.75. An uncooled vane of the same aerodynamic design was also tested to provide a base point for comparison of the cooled vane performance. The following results were obtained:

1. The primary flow decreased with increasing coolant flow for both cooled vanes. The rate of decrease was 1.0 percent per percent coolant flow for the convection-film-cooled vane and 2.0 percent per percent coolant flow for the transpiration cooled vane. At a coolant to primary pressure ratio of 1.0 and a primary to coolant temperature ratio of 2.76 the primary flow for the transpiration cooled vane was 7.0 percent less than it was for the uncooled vane. The coolant flow for these conditions was 3.5 percent of the primary flow. The corresponding figures for the convection-film-cooled vane were

a 4.4 percent reduction in primary flow with a coolant flow of 3.6 percent of the primary flow.

2. The primary efficiency of the convection-film-cooled blade increased with increased coolant flow and was also dependent on the primary to coolant temperature ratio. The highest primary efficiencies occurred at a temperature ratio of 1.0 and the lowest at a temperature ratio of 2.75. The primary efficiency of the transpiration-cooled vane decreased with increased coolant flow and was not dependent on the temperature ratio. Both of these effects were attributed to the manner in which the coolant was injected into the primary flow. The convection-film-cooled vane ejected the coolant substantially in the direction of the primary flow. In this case the energy of the coolant could add to the output of the vane. The transpiration-cooled vane ejected the coolant normal to the direction of the primary flow so that the energy of the coolant could not be effectively utilized.

3. At a coolant to primary pressure ratio of 1.0 and a primary to coolant temperature ratio of 2.75 the primary efficiency of the convection-film-cooled vane was 0.951 compared to 0.918 for the transpiration-cooled vane at similar conditions. At these same conditions, the thermodynamic efficiencies were 0.939 for the convection-film-cooled vane and 0.907 for the transpiration cooled vane. The efficiency of the uncooled vane was 0.954.

Lewis Research Center,

National Aeronautics and Space Administration,

Cleveland, Ohio, November 8, 1972,

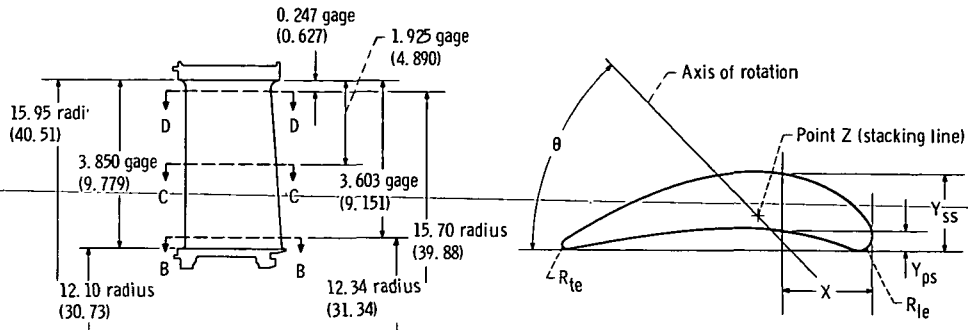
501-24.

REFERENCES

1. Moffitt, Thomas P.; Prust, Herman W., Jr.; Szanca, Edward M.; and Schum, Harold J.: Summary of Cold-Air Tests of a Single-Stage Turbine with Various Stator Cooling Techniques. NASA TM X-52968, 1971.
2. Prust, Herman W., Jr.: An Analytical Study of the Effect of Coolant Flow Variables on the Kinetic Energy Output of a Cooled Turbine Blade Row. NASA TM X-67960, 1971.
3. Calvert, Howard F.; Cochran, Reeves P.; Dengler, Robert P.; Hickel, Robert O.; and Norris, James W.: Turbine Cooling Research Facility. NASA TM X-1927, 1970.
4. Gladden, Herbert J.; Dengler, Robert P.; Evans, David G.; and Hippensteele, Steven A.: Aerodynamic Investigation of Four-Vane Cascade Designed for Turbine Cooling Studies. NASA TM X-1954, 1970.

TABLE I - VANE SECTION DATA

[All dimensions are in inches (cm) unless otherwise indicated.]



Section	B-B		C-C		D-D	
Point X	1.039		1.028		1.012	
Z Y	0.261		0.333		0.404	
θ	28°46'		33°33'		38°20'	
R_{le}	0.160		0.160		0.160	
R_{te}	0.035		0.034		0.033	
X	Y_{ps}	Y_{ss}	Y_{ps}	Y_{ss}	Y_{ps}	Y_{ss}
0.000	0.160	0.160	0.160	0.160	0.160	0.160
.100	-----	.319	-----	.323	-----	.337
.200	.005	.390	.006	.408	.006	.429
.300	.043	.450	.050	.473	.057	.495
.400	.077	.497	.093	.523	.108	.543
.500	.105	.536	.127	.560	.148	.576
.600	.132	.566	.156	.587	.177	.601
.700	.156	.587	.180	.606	.199	.619
.800	.177	.601	.197	.619	.214	.630
.900	.194	.610	.211	.624	.227	.633
1.000	.207	.611	.222	.624	.235	.631
1.100	.216	.606	.231	.619	.240	.624
1.200	.221	.535	.235	.608	.243	.612
1.300	.224	.580	.236	.590	.242	.584
1.400	.223	.560	.233	.568	.238	.571
1.500	.220	.534	.227	.541	.228	.542
1.600	.212	.503	.217	.508	.217	.507
1.700	.201	.467	.205	.472	.202	.470
1.800	.186	.426	.188	.431	.183	.427
1.900	.167	.382	.168	.334	.161	.380
2.000	.144	.334	.144	.334	.137	.328
2.100	.118	.283	.115	.280	.110	.274
2.200	.087	.229	.083	.223	.081	.215
2.300	.055	.171	.048	.162	.046	.155
2.400	.020	.112	.012	.098	.009	.091
2.460	-----	-----	-----	.033	.033	.033
2.470	-----	-----	.034	.034	-----	-----
2.493	.035	.035	-----	-----	-----	-----

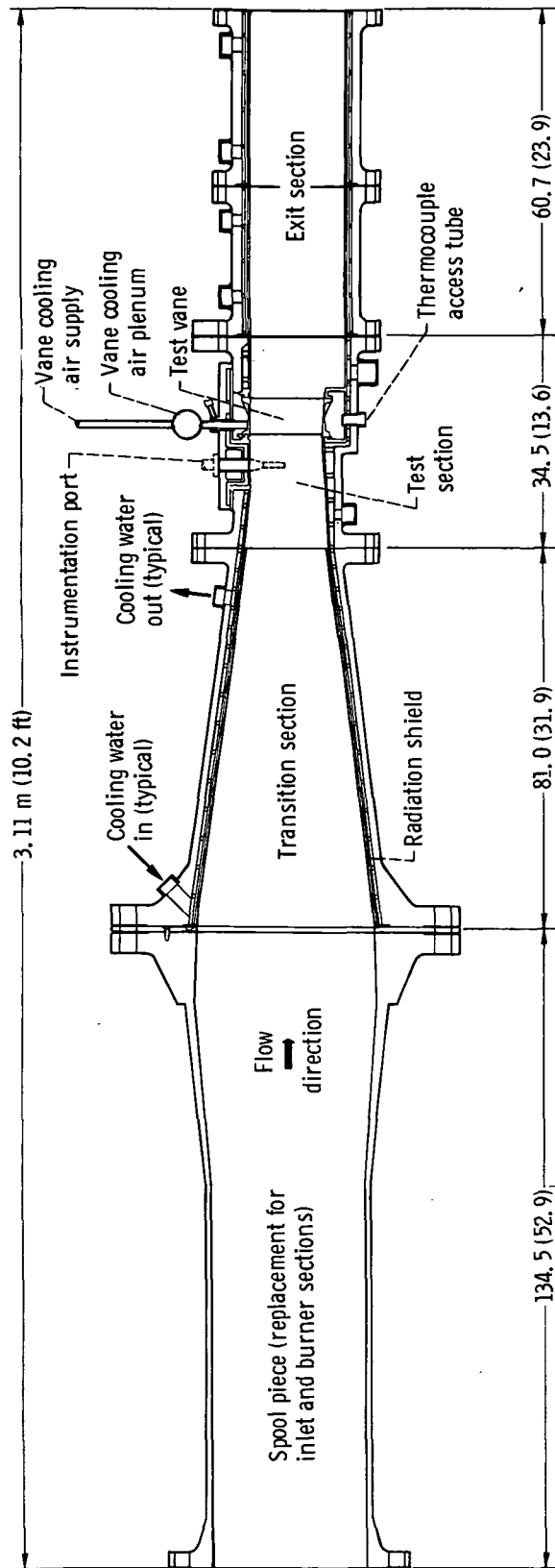


Figure 1. - Schematic cross-sectional view of modified basic test unit of cascade facility. (All dimensions in cm (in.) unless otherwise indicated.)

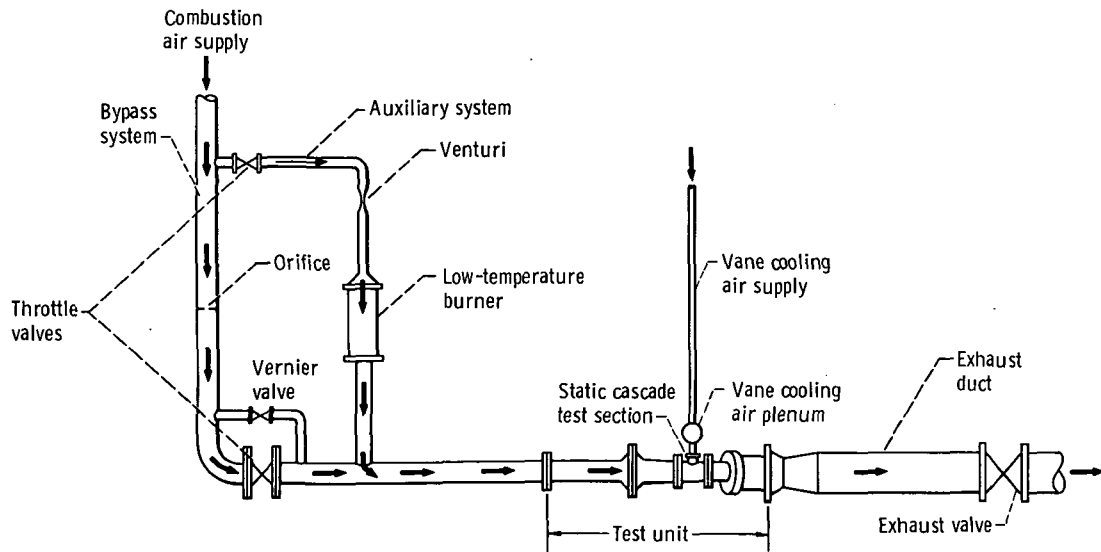


Figure 2. - Schematic view of cascade facility.

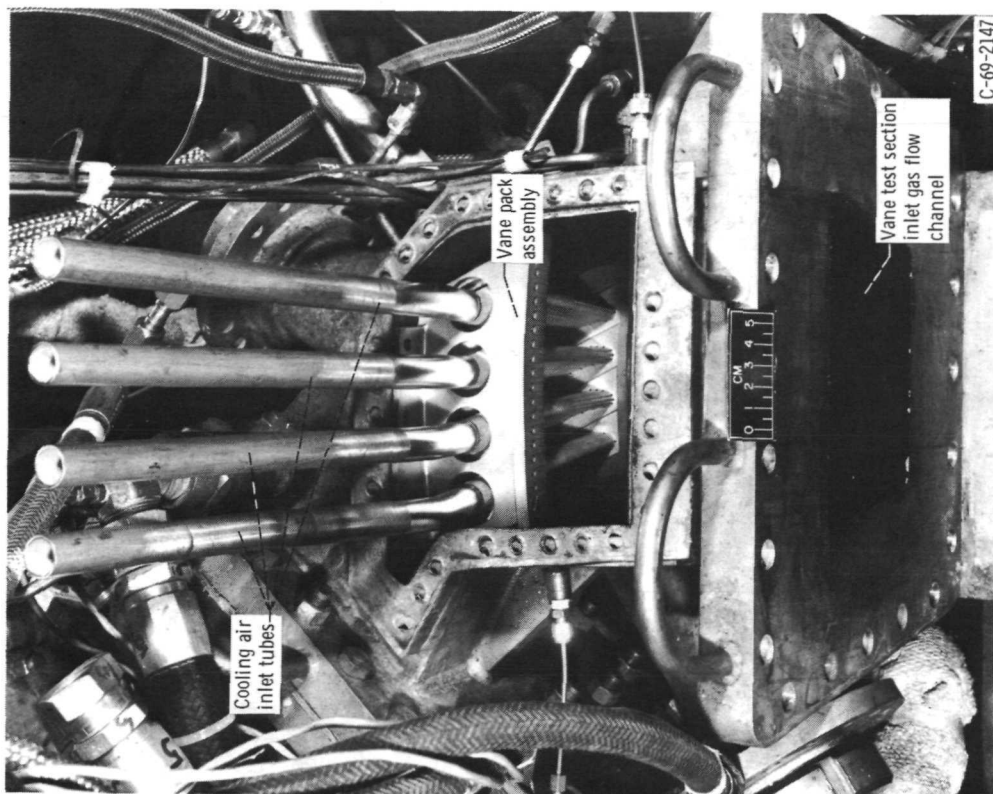


Figure 4. - Top view of cascade test section with access cover removed.

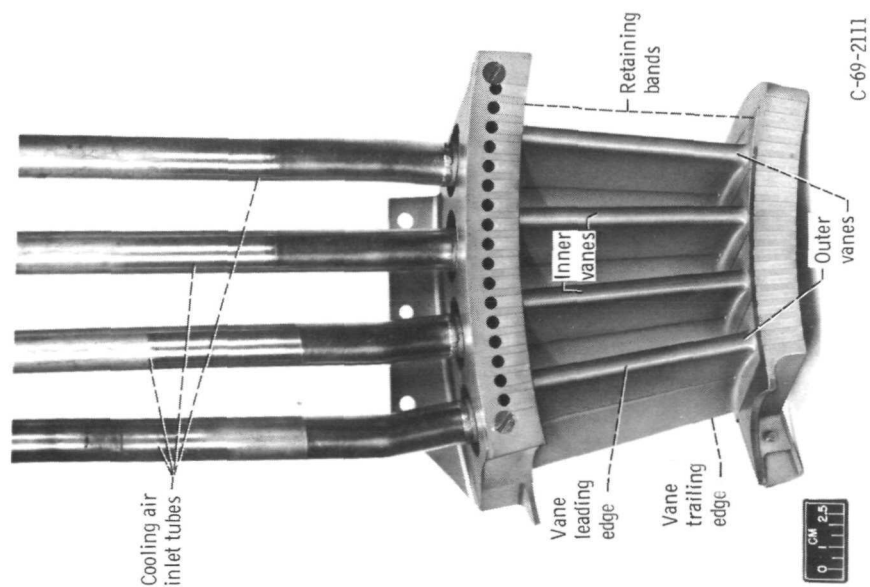


Figure 3. - Typical vane pack.

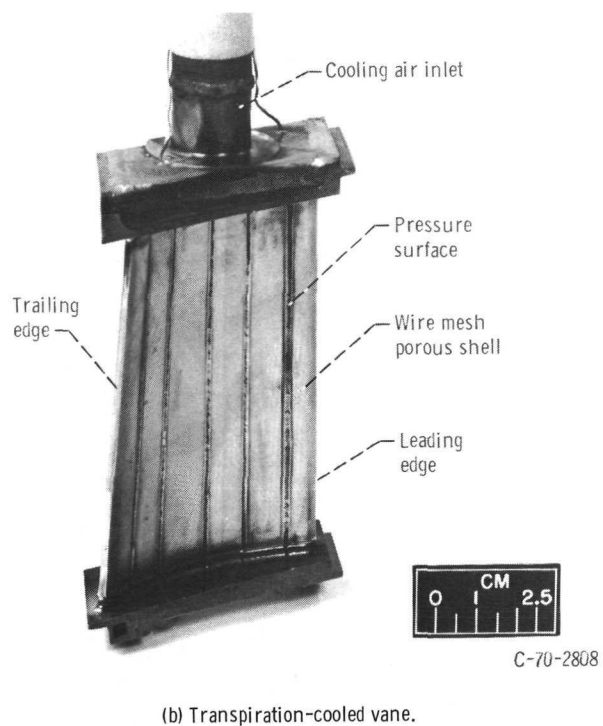
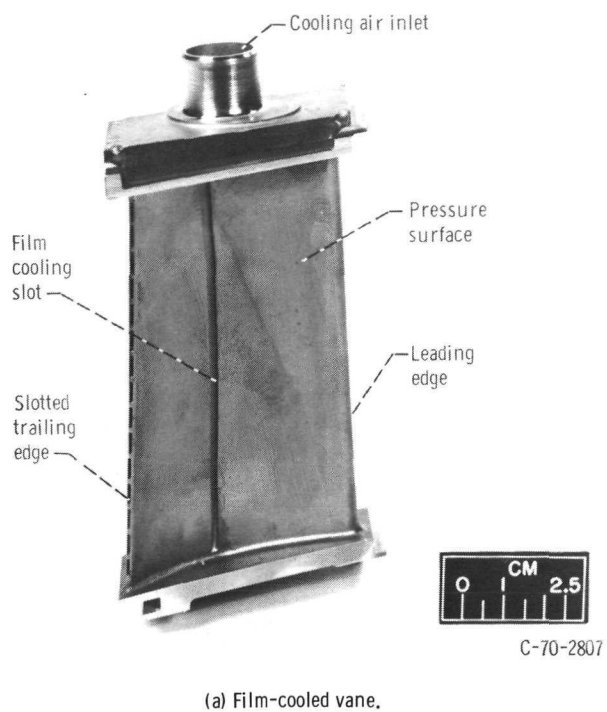
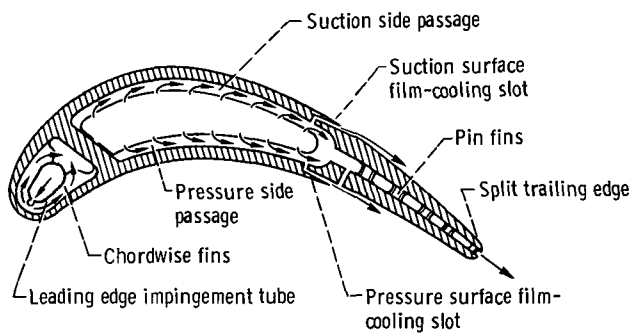


Figure 5. - Air-cooled turbine vanes.



Section A-A

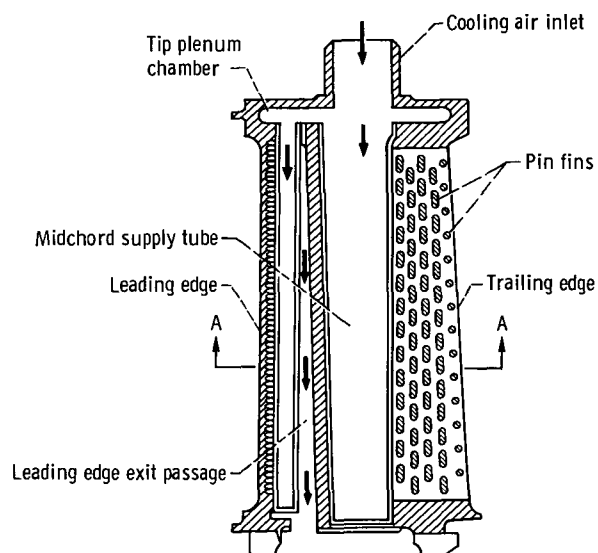
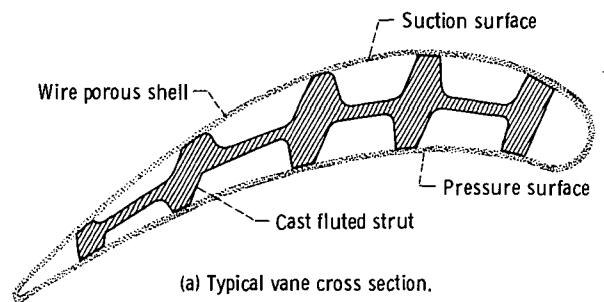
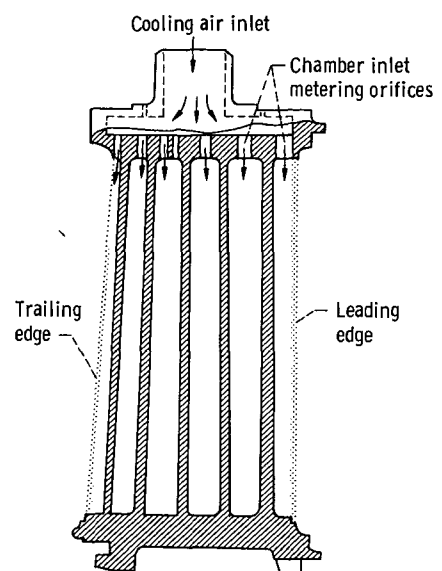


Figure 6. - Film-cooled vane internal flow configuration.

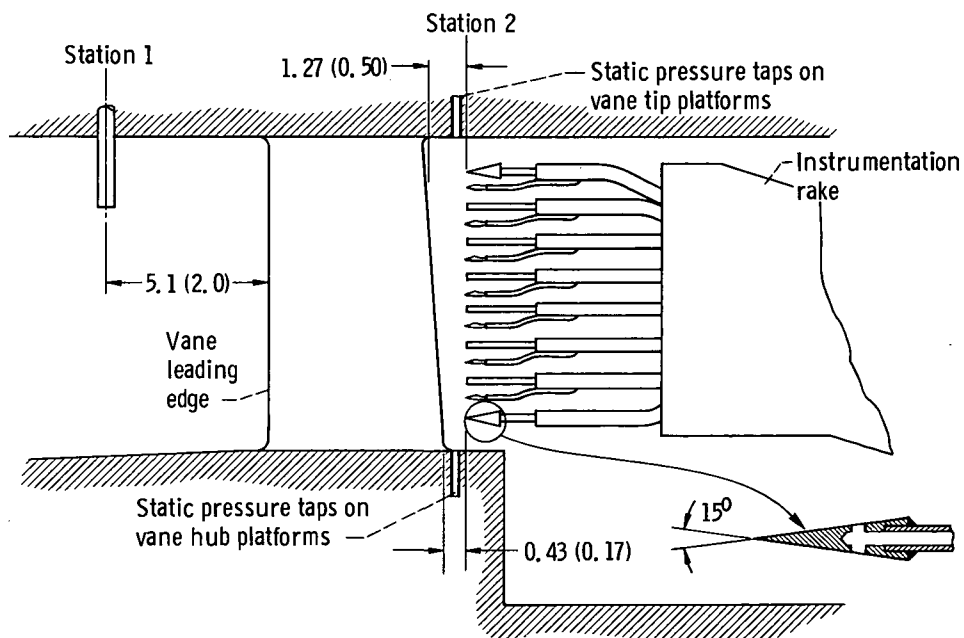
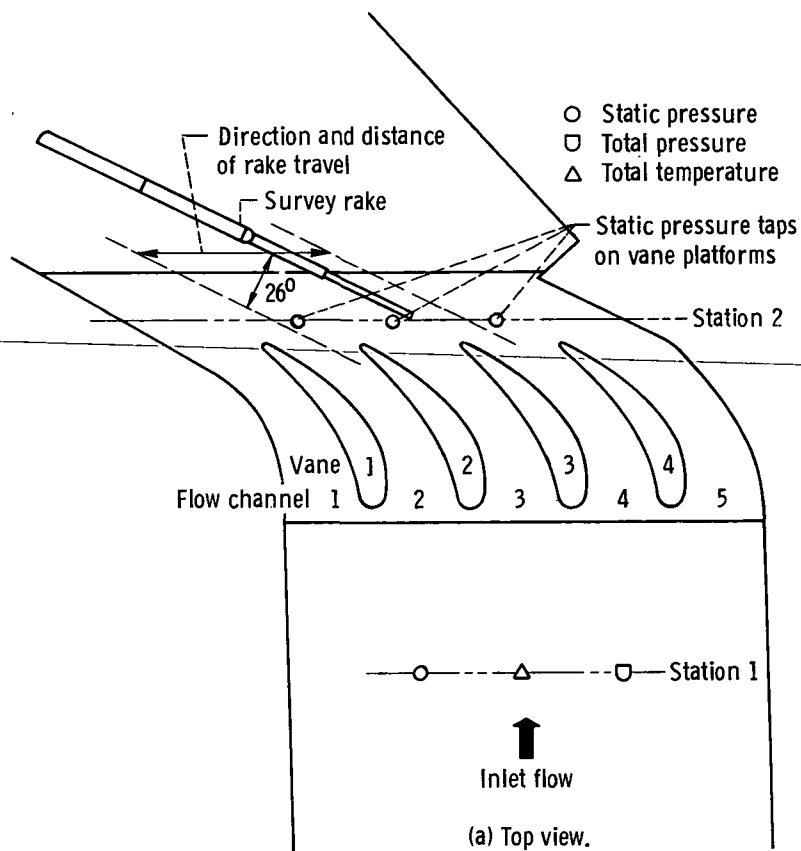


(a) Typical vane cross section.



(b) Pressure surface.

Figure 7. - Transpiration-cooled vane internal flow configuration.



(b) Side view. (All dimensions in cm (in.) unless indicated otherwise.)

Figure 8. - Schematics of vane test section showing pertinent instrumentation.

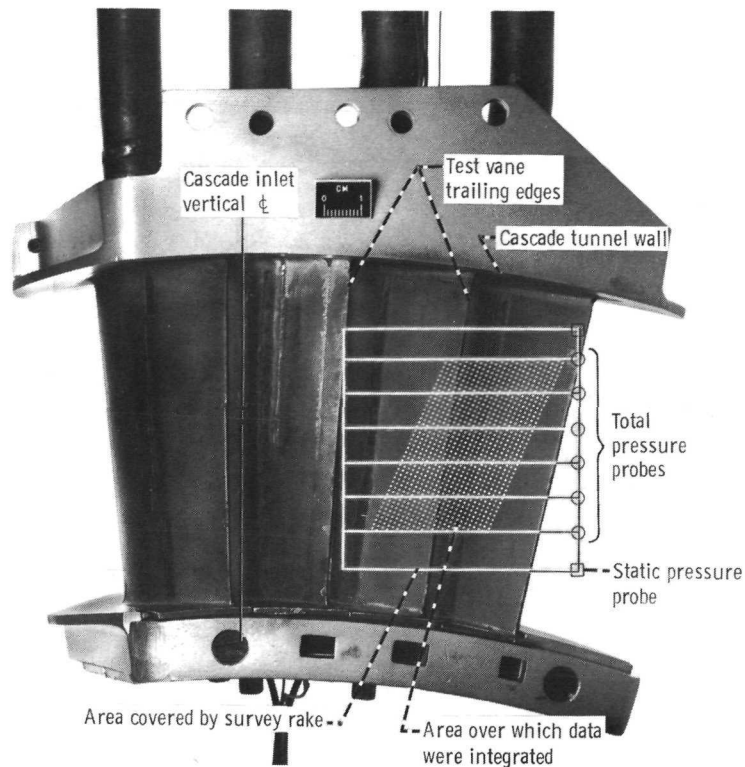


Figure 9. - Sketch of cascade exit showing vane trailing edges area covered by survey rake, and area over which data were integrated.

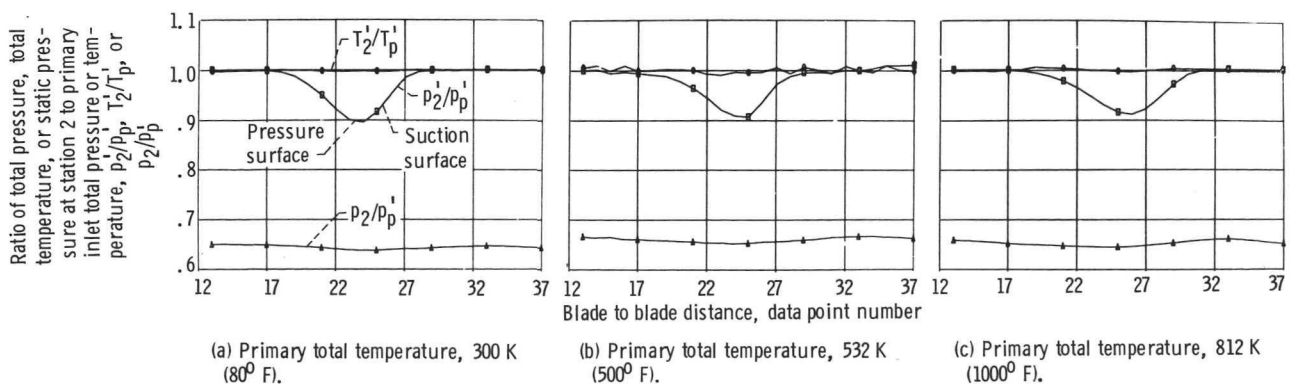


Figure 10. - Blade to blade variation of total pressure, static pressure, and total temperature at station 2 for uncooled vanes.

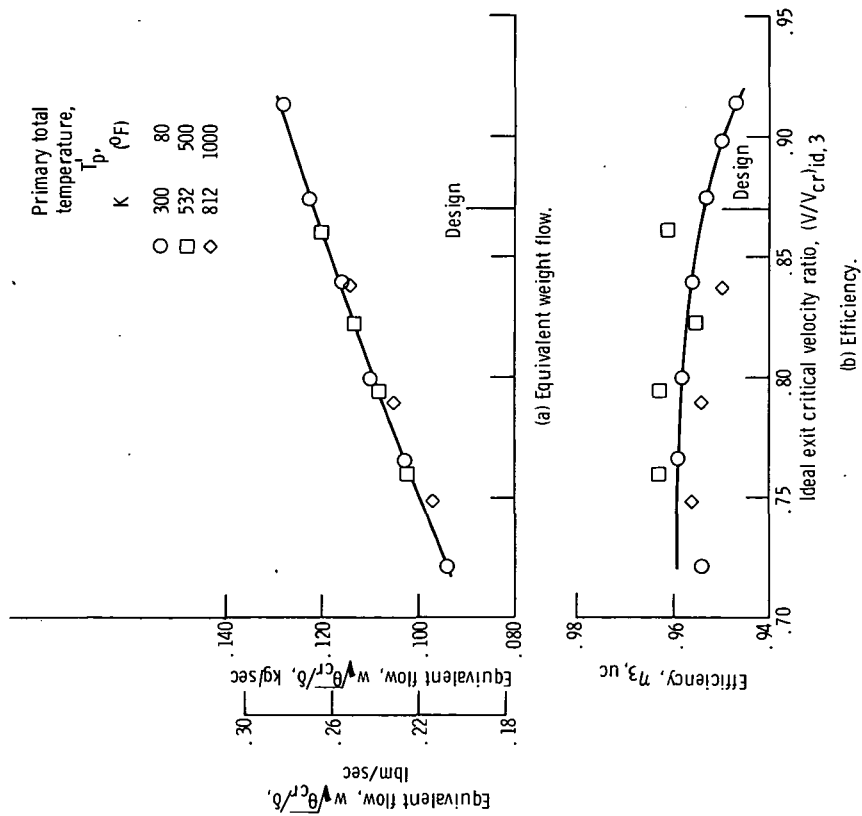


Figure 11. - Variation of equivalent weight flow and efficiency with ideal exit critical velocity ratio for uncooled vanes.

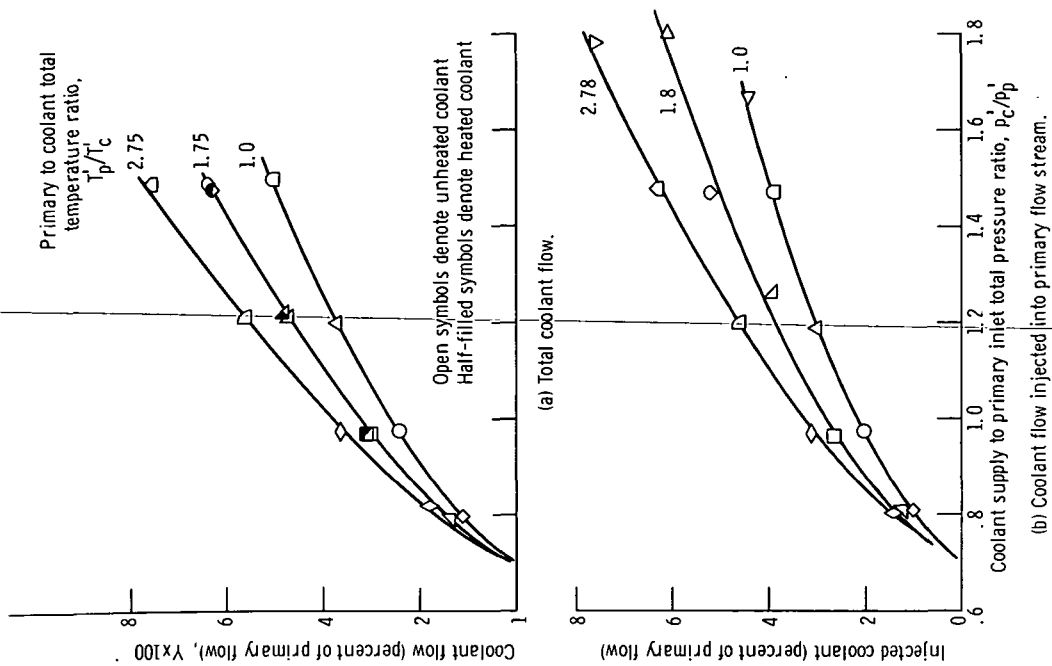


Figure 12. - Variation of coolant flow with coolant pressure and temperature ratio for convection-film-cooled vanes.

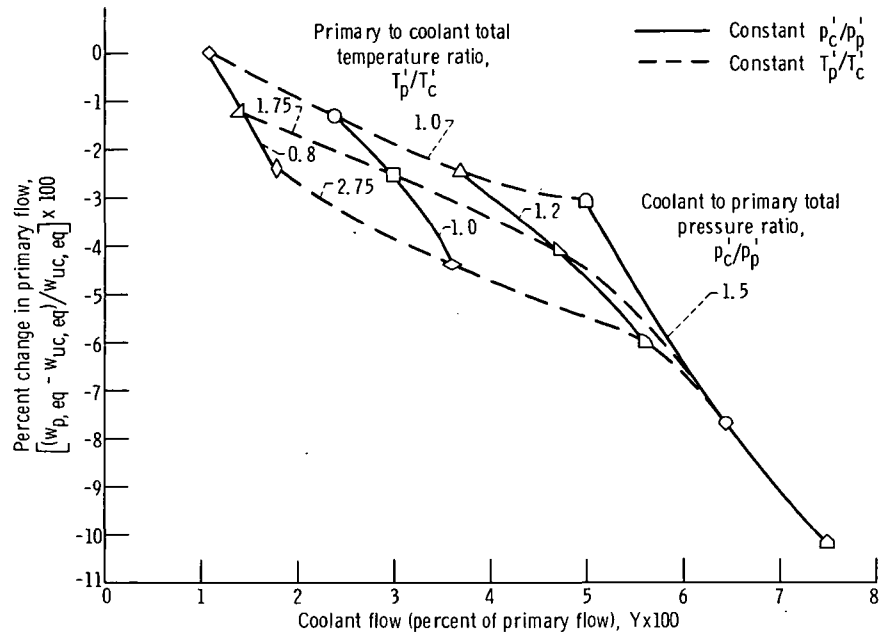


Figure 13. - Change in primary flow with coolant flow for convection-film-cooled vanes.

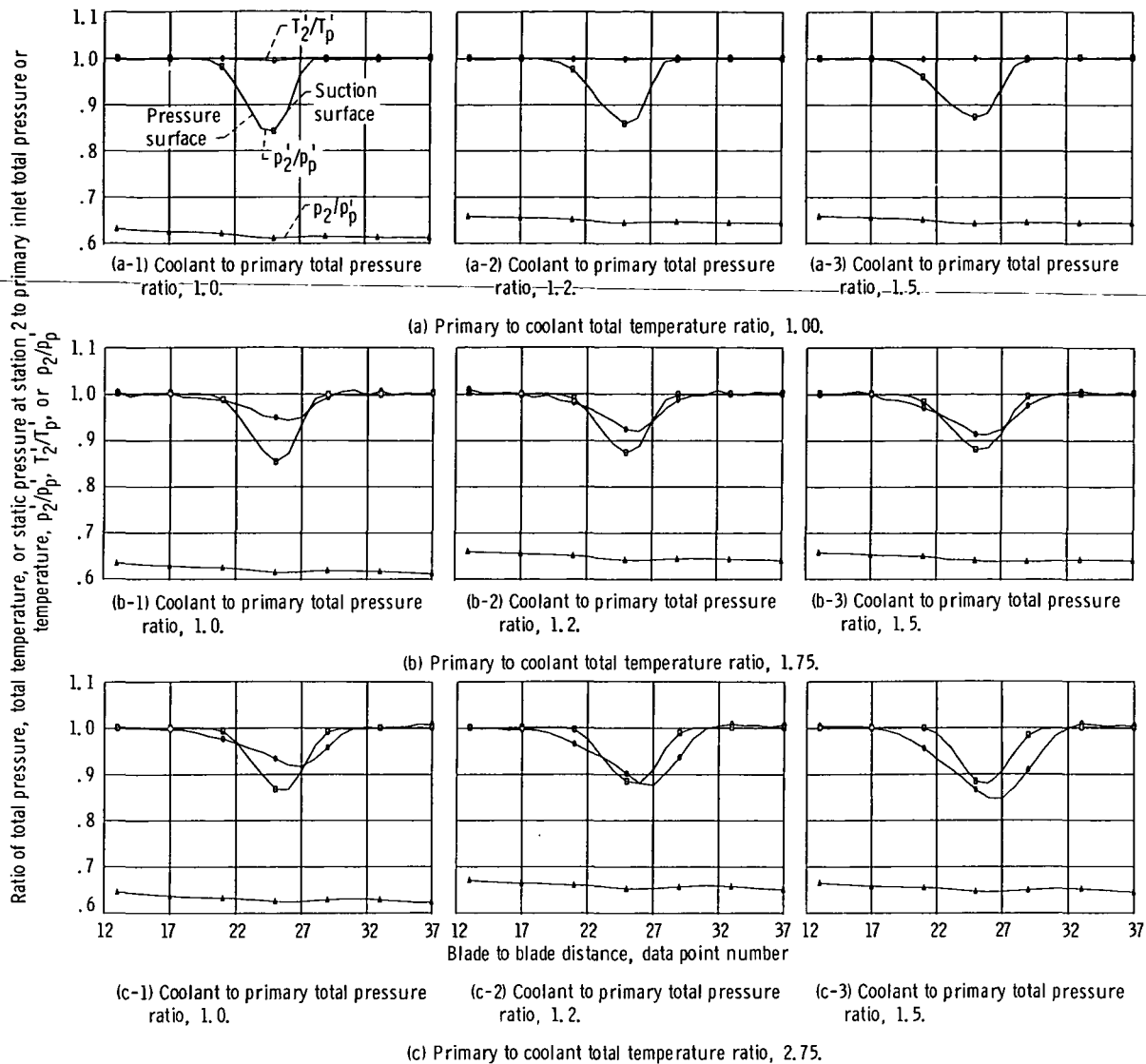


Figure 14. - Blade to blade variation of total pressure, static pressure, and total temperature at station 2 for convection-film-cooled vanes.

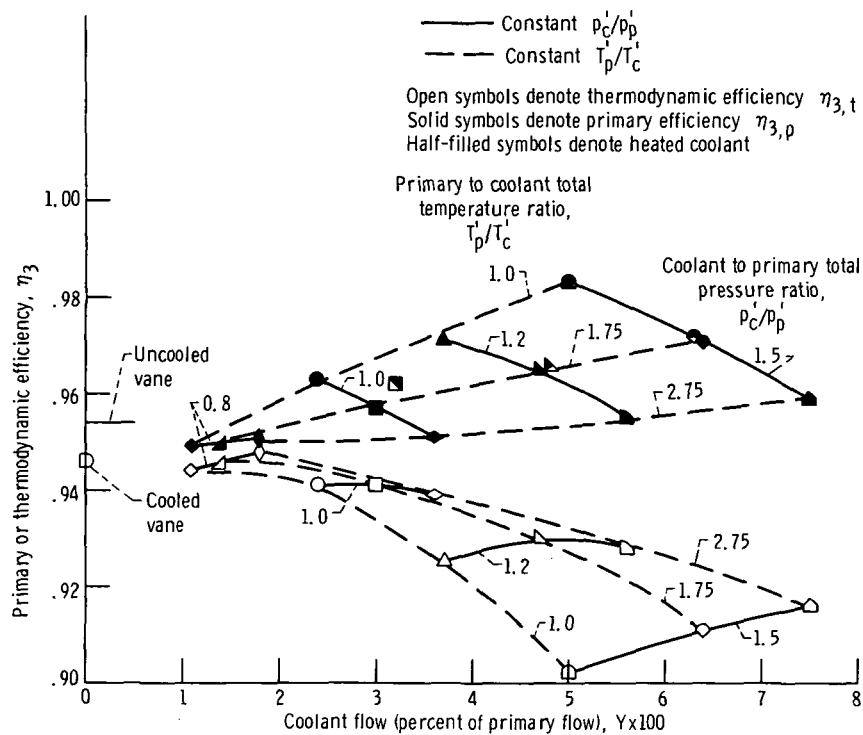


Figure 15. - Primary and thermodynamic efficiency for convection-film-cooled vanes.

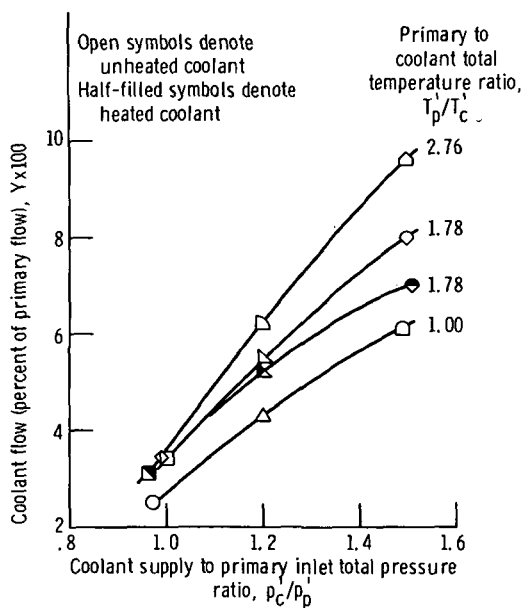


Figure 16. - Variation of coolant flow with coolant pressure and temperature ratios for transpiration-cooled vanes.

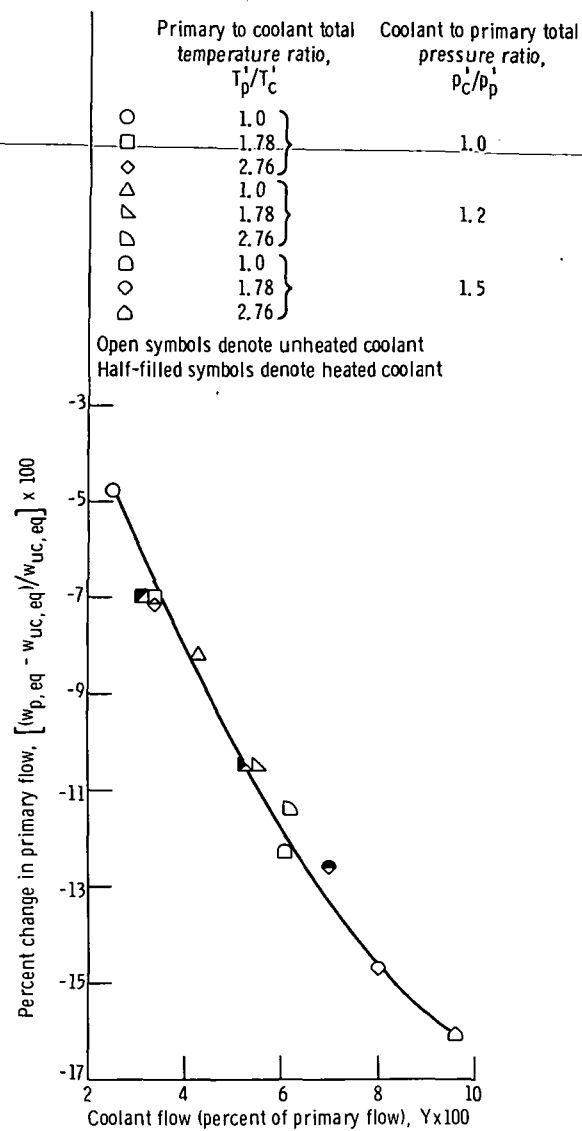


Figure 17. - Change in primary flow with coolant flow for transpiration-cooled vanes.

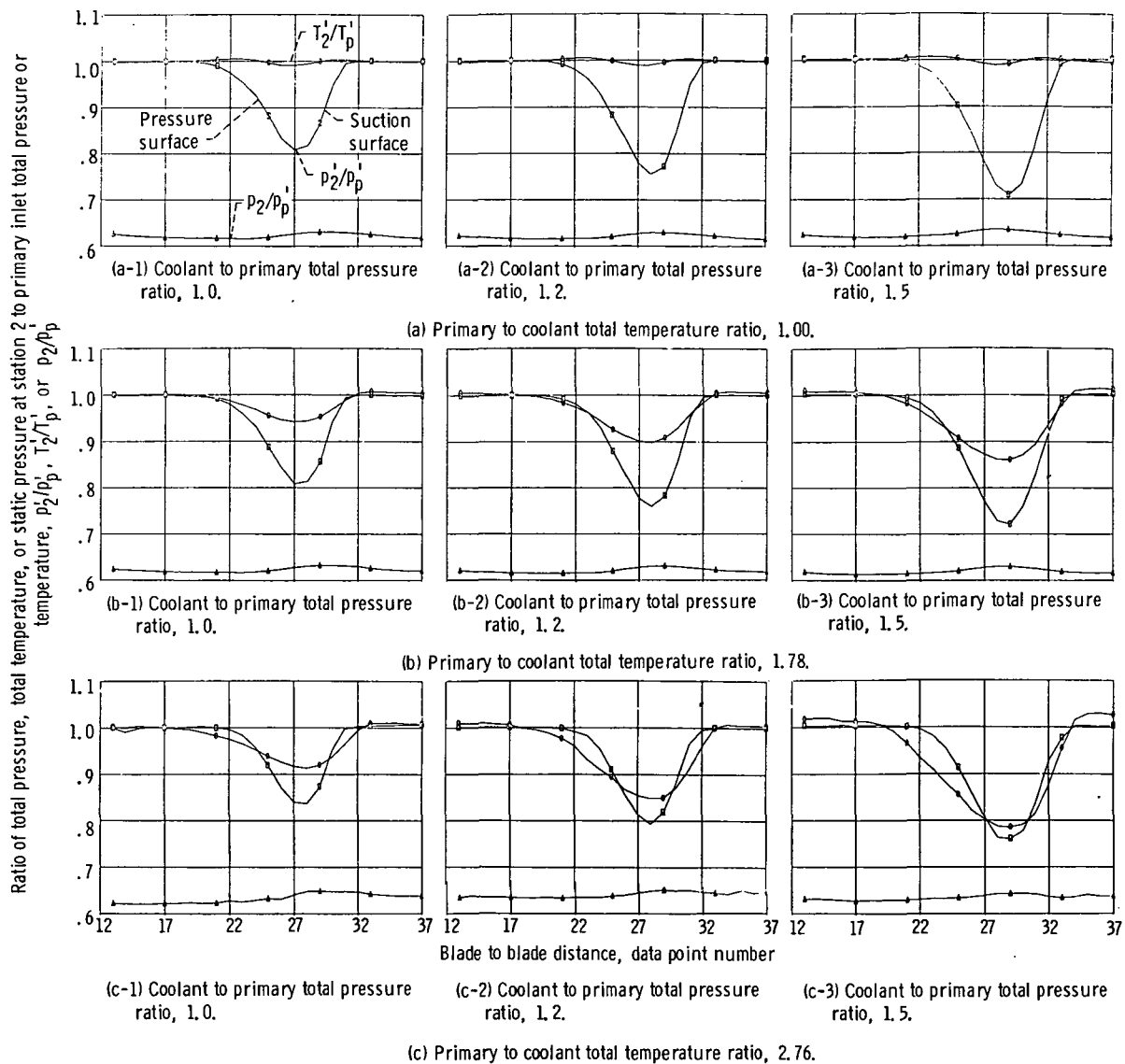


Figure 18. - Blade to blade variation of exit total pressure, static pressure, and total temperature for transpiration-cooled vanes.

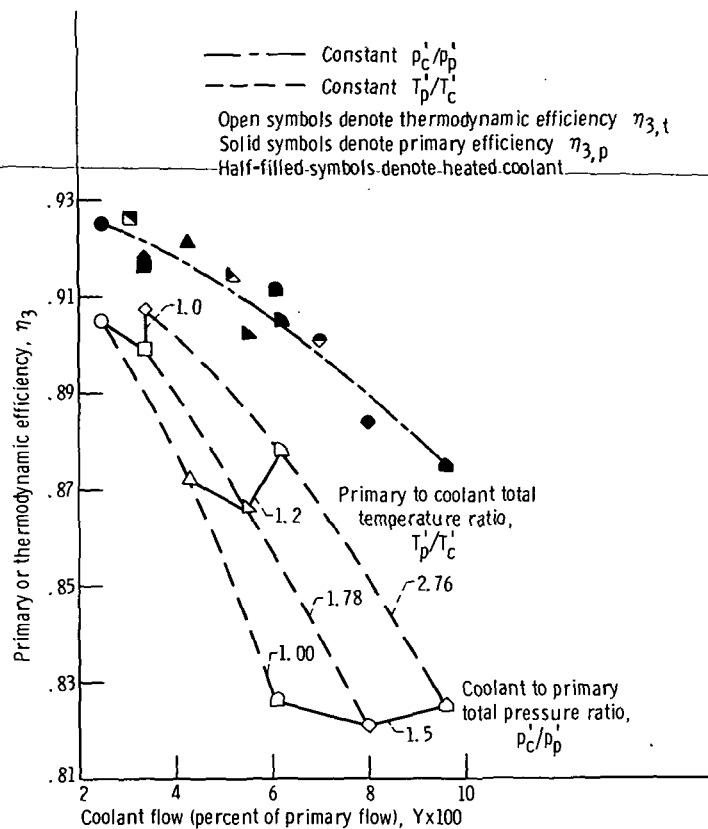


Figure 19. - Primary and thermodynamic efficiency for transpiration-cooled vanes.

Page Intentionally Left Blank



POSTMASTER:

If Undeliverable (Section 158
Postal Manual) Do Not Return

"The aeronautical and space activities of the United States shall be conducted so as to contribute . . . to the expansion of human knowledge of phenomena in the atmosphere and space. The Administration shall provide for the widest practicable and appropriate dissemination of information concerning its activities and the results thereof."

—NATIONAL AERONAUTICS AND SPACE ACT OF 1958

NASA SCIENTIFIC AND TECHNICAL PUBLICATIONS

TECHNICAL REPORTS: Scientific and technical information considered important, complete, and a lasting contribution to existing knowledge.

TECHNICAL NOTES: Information less broad in scope but nevertheless of importance as a contribution to existing knowledge.

TECHNICAL MEMORANDUMS: Information receiving limited distribution because of preliminary data, security classification, or other reasons. Also includes conference proceedings with either limited or unlimited distribution.

CONTRACTOR REPORTS: Scientific and technical information generated under a NASA contract or grant and considered an important contribution to existing knowledge.

TECHNICAL TRANSLATIONS: Information published in a foreign language considered to merit NASA distribution in English.

SPECIAL PUBLICATIONS: Information derived from or of value to NASA activities. Publications include final reports of major projects, monographs, data compilations, handbooks, sourcebooks, and special bibliographies.

TECHNOLOGY UTILIZATION PUBLICATIONS: Information on technology used by NASA that may be of particular interest in commercial and other non-aerospace applications. Publications include Tech Briefs, Technology Utilization Reports and Technology Surveys.

Details on the availability of these publications may be obtained from:

SCIENTIFIC AND TECHNICAL INFORMATION OFFICE

NATIONAL AERONAUTICS AND SPACE ADMINISTRATION

Washington, D.C. 20546